

12th Deep Sea Offshore Wind R&D Conference, EERA DeepWind'2015

Probabilistic fatigue analysis of jacket support structures for offshore wind turbines exemplified on tubular joints

Sebastian Kelma*, Peter Schaumann

ForWind Hannover, Institute for Steel Construction, Leibniz University Hannover, 30167 Hannover, Germany

Abstract

The design of offshore wind turbines is usually based on the semi-probabilistic safety concept. Using probabilistic methods, the aim is to find an advanced structural design of OWTs in order to improve safety and reduce costs. The probabilistic design is exemplified on tubular joints of a jacket substructure. Loads and resistance are considered by their respective probability distributions. Time series of loads are generated by fully-coupled numerical simulation of the offshore wind turbine. Especially the very high stress ranges that rarely occur during a period with constant conditions are decisive for the fatigue design. The peak-over-threshold method is applied to find the probability distribution of the very high stress ranges. The method of maximum-likelihood estimation is used to determine the parameters of the underlying generalized Pareto distribution. Further analysis shows that especially the number of the very high stress ranges, scattering for different time series, has a significant impact on the resulting fatigue damage.

© 2015 The Authors. Published by Elsevier Ltd. This is an open access article under the CC BY-NC-ND license (<http://creativecommons.org/licenses/by-nc-nd/4.0/>).

Peer-review under responsibility of SINTEF Energi AS

Keywords: offshore wind energy; jacket substructure; tubular joints; fatigue design; probabilistic analysis; peak-over-threshold method; generalized Pareto distribution

1. Introduction

Jackets are commonly used substructures of offshore wind turbines (OWTs) with a rated power of at least 5 MW for sites with water depths as from 25 m. During their life time, OWTs and the used substructures are stressed by

* Corresponding author. Tel.: +49-511-762-4139; fax: +49-511-762-2991.
E-mail address: kelma@stahl.uni-hannover.de

fatigue loads caused by wind, operation, and sea state. Especially the welded tubular joints of jackets are highly stressed due to their complex geometry.

The design of support structures is usually based on the semi-probabilistic safety concept, as defined in standards such as DNV-OS-J101 [1]. Instead, the probabilistic safety concept can be applied for an improved design of jacket substructures [2]. For that purpose, adequate and accurate description of the stochastic behavior of load effects, loads, and resistance shall be available. Predictions of loads acting on the OWT are commonly derived from numerical simulations. The aim is to find an advanced design of OWTs by applying probabilistic safety concept. Hence, cost of support structures for OWTs can be reduced. In general, probabilistic design of OWTs still is a topic of research [3] [4].

2. Fatigue design of offshore wind turbines

2.1. Semi-probabilistic design

Within the semi-probabilistic safety concept, cf. e.g. DNV-OS-J101 [1], characteristic values of loads S_k and resistance R_k are chosen as specific quantiles of their respective probability distributions. Uncertainties of the characteristic values are covered by load and material factors, γ_f and γ_m . The resulting design value for the load S_d must not exceed the design value of the resistance R_d . This general limit state to be fulfilled is given by Eq. (1). Load and material factor can be adapted in order to cover certain safety levels and consequence classes of failure.

$$S_d = \gamma_f \cdot S_k \leq \frac{R_k}{\gamma_m} = R_d \quad (1)$$

When considering fatigue, the characteristic value R_k of the S-N curve is defined as the mean value minus two-times the standard deviation of the underlying distribution of the detail category $\Delta\sigma_c$ for the endurance of $2 \cdot 10^6$, cf. DNVGL-RP-0005 [5]. The stress ranges (loads) are found by numerical simulation of OWTs affected by environmental conditions as defined in design load cases, cf. e.g. IEC 61400-3 [6]. The statistical combination of the parameters describing these conditions usually is stated in the design basis of the planned OWT. The fatigue damage is calculated by applying Palmgren-Miner's rule,

$$D_{fat} = \sum_i \frac{n(\Delta\sigma_i)}{N_{Ri}(\Delta\sigma_i)} \leq \eta \quad (2)$$

where n is the number of stress ranges with the value $\Delta\sigma$, and N_R is the corresponding endurance for the stress range. The accounted fatigue damage D_{fat} shall not exceed a certain value of the usage factor η , as named in DNVGL-RP-0005 [5]. Its value depends on the accessibility of the structural member for inspections.

For the semi-probabilistic fatigue design as required by IEC 61400-3 [6], only six numerical simulations of the OWT with a duration of ten minutes and different wind seeds and sea states are required for each wind speed being considered. Recent studies on the joints of a jacket structure [7] with a 5 MW wind turbine by Zwick and Muskulus [8] show that an error of up to 12% for fatigue loads can occur with a probability of 1% for simulations with a total duration of 60 minutes, resulting in an overestimation of the fatigue life by up to 29%.

2.2. Probabilistic design

For safety verification when using the probabilistic safety concept, the probability that the loads are greater than the resistance must not exceed a predefined value for the probability of failure. A value for the probability of failure of 10^{-4} for unmanned OWTs represents the normal safety class, as stated in DNV-OS-J101 [1]. Generally, target reliabilities shall be chosen such that they "commensurate with the consequence of failure" [1].

When applying the probabilistic design, all possible load scenarios are to be considered. Considering the high number of environmental conditions for all possible operational states of OWTs during the life time, the required

effort is significantly increased compared to the semi-probabilistic design. Instead of choosing characteristic parameters, the respective probability distributions of load effects, loads, and resistances are taken into account.

For the probabilistic fatigue design, Palmgren-Miner's rule, cf. to Eq. (2), has to be rephrased in order to cover the underlying probability distributions of load effects, loads, and resistance. The expected fatigue damage is given by Eq. (3), which has been developed by the authors. Degradation of resistance over the life time of the OWT is to be considered. Within the integral in Eq. (3), degradation and distribution of load effects over time are represented by the variable *LT* ('life time'). *n* is the total number of stress ranges within the considered time period.

$$D_{fat} = \int_{life\ time} \iint \frac{n \cdot f(\Delta\sigma, LT)}{N(\Delta\sigma | \Delta\sigma_c)} \cdot g(\Delta\sigma_c) \cdot d\Delta\sigma \cdot d\Delta\sigma_c \cdot dLT \leq D_{cr} \tag{3}$$

Scattering of both loads and resistance is described by the probability density functions $f(\Delta\sigma)$ and $g(\Delta\sigma_c)$, respectively. While the scattering of the fatigue resistance $\Delta\sigma_c$ is well known, cf. section 2.3, the stochastic description of stress ranges $\Delta\sigma$ acting on the structural component is more complex. The following investigations concentrate on the scattering of loads and resistance for a specified reference scenario. Scattering of the critical fatigue damage D_{cr} follows a lognormal distribution with a mean value of unity and a variance of 0.3, according to the Joint Committee on Structural Safety (JCSS) [9].

Probabilistic fatigue design for tubular joints of tripod substructures already was carried out by Thöns [4], with the focal point being set on the modeling of fatigue resistance and its scatter. Within [4], the probability distributions of fatigue loads are assumed to be Weibull-distributed.

2.3. Fatigue resistance of steel components

The fatigue resistance is given by S-N curves, setting stress ranges and endurable number of load cycles into relation. In log-log coordinate systems, S-N curves consist of several linear sections. For steel components, all S-N curves have the same shape. The respective fatigue strength, depending on the component, is defined by the detail category $\Delta\sigma_c$, which is the stress range at an endurable number of load cycles of $2 \cdot 10^6$.

Material-related scattering of fatigue strength is detected by evaluating of fatigue tests. The fatigue strength can be described by a lognormal distribution, as stated by e.g. the JCSS [9]. A collection of data of fatigue tests is given by e.g. Sonsino et al. [10]. Here, stress ranges of several fatigue test series, normalized by their respective detail categories, are summarized. The normalized test data are adopted such that the characteristic value for the detail category is 90 MPa. The adopted test data are shown in Fig. 1 (blue dots).

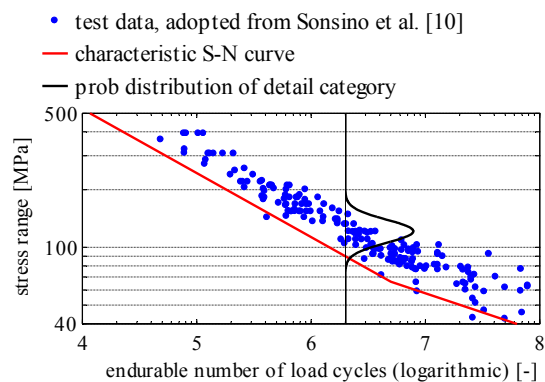


Fig. 1. Fatigue test data S-N curve for steel components with detail category of 90 MPa.

Further investigation of the test data shows that the detail category $\Delta\sigma_c$ is lognormal-distributed with a mean value of 125 MPa and a standard deviation of 17.5 MPa. This distribution is plotted in Fig. 1 (black line), as well as the respective characteristic S-N curve with the characteristic fatigue resistance of 90 MPa (red line).

3. Numerical simulation of reference offshore wind turbine

3.1. Reference load scenario and reference structure

Only one reference load scenario is considered in order to demonstrate the principle of probabilistic fatigue design. Here, a load scenario is chosen in accordance to the design load case DLC 1.2, c.f. IEC 61400-3 [6].

The OWT in operation is affected by a turbulent wind field and an irregular sea state (Fig. 2 (a)). Within the study, seeds of turbulent wind fields with mean value of 12 ms^{-1} and a turbulence intensity of 14 % at hub height of the OWT are applied. The exponential wind shear factor is 0.14. To describe the irregular sea state, the JONSWAP spectrum with a significant wave height of 2.5 m and a peak period of 7.5 s is applied. Wave spreading is not considered. The propagation of wind and waves is parallel to the diagonal of the jacket's foot print.

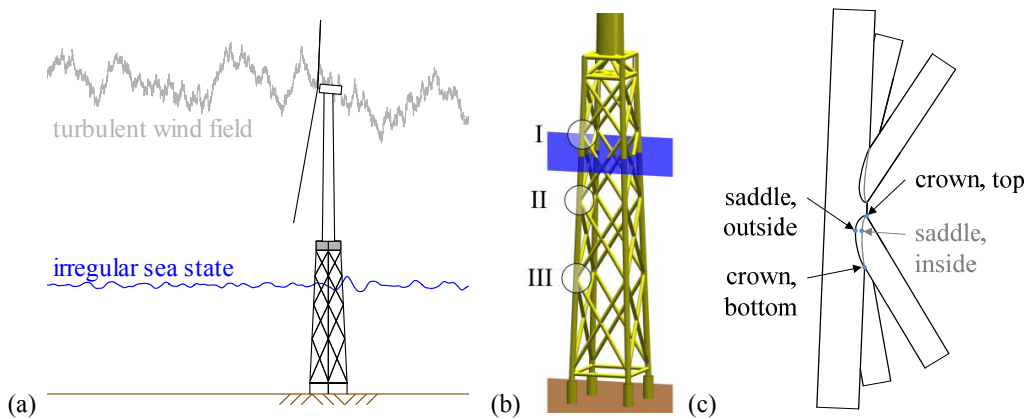


Fig. 2. (a) OWT effected by wind and waves; (b) jacket substructure; (c) tubular joint.

The model of the OWT consists of the NREL 5 MW turbine [11] with a nominal hub height of 90.55 m above mean sea level as well as the jacket substructure as defined within the OC4 project [7]. The jacket is designed for a site in the North Sea with a water depth of 50 m. Chords and braces are tubes with diameters of 1.20 m and 0.8 m, respectively. The jacket structure as well as the K-joints considered in this study are shown in Fig. 2 (b).

Within the study, the structural stress approach is applied for calculation of the stress acting at the K-joints of the jacket structure. The stress due to the branched geometry of the tubular joints is given by multiplying the occurring nominal stress by stress concentration factors (SCFs). For each brace of the considered K-joints, SCFs for crown (top and bottom) and saddle (inside and outside) are calculated, applying the formulae given by Efthymiou [12]. The positions of the SCFs are visualized in Fig. 2 (c).

3.2. Numerical simulation

Fully-coupled simulations of the OWT with jacket substructure are carried out. The wind-induced loads are computed by using the widely-used wind-energy simulation program Flex5, which is coupled with the FE tool Poseidon [13]. Poseidon is specialized on the calculation of wave-induced loads.

53 numerical simulations with a duration of 3600 seconds for the OWT with different wind seeds and irregular sea states are carried out. The number and length of the time series is chosen such that a sufficiently high number of data are available as it is required for the stochastic analyses carried out.

The stress ranges for the fatigue design are determined by applying the rainflow-counting algorithm on each of the time series for each structural component considered. Full and half hysteresis loops (called cycles in the following) are found. Only full cycles are considered for further investigations.

Investigations concentrate on the fatigue design of the upper brace of the K-joint III (crown-bottom), which is the most critical spot considering fatigue. The procedures described in the following can also be applied on the other hot spots, as further investigations have shown, which are not presented in this paper.

4. Statistical analysis of fatigue damage determined with the semi-probabilistic safety concept

Each of the time series for the upper brace of the K-joint III (crown-bottom) is evaluated concerning its fatigue damage, using the semi-probabilistic safety concept. A S-N curve with characteristic detail category of 90 MPa is applied. The fatigue damage differs for each time series of 3600 seconds. This scattering can be described by the ratio of standard deviation to mean value of the fatigue damages with a value of 18 %. The 53 values of fatigue damage normalized by the mean value lie in the range of about -26 % up to about +46 %. In order to explain the scattering, the empirical cumulative distribution functions (CDFs) of stress ranges are plotted in Fig. 3 (a). As can be seen, the curves of CDFs of time series scatter (blue lines). This eventually results in different values of fatigue damage.

In order to underline the importance of the very high stress ranges, the relative cumulative fatigue damage of full cycles is shown in Fig. 3 (b). The relative cumulative fatigue damage $D_{fat,cum,rel}$ is defined as

$$D_{fat,cum,rel}(\Delta\sigma) = \frac{1}{D_{fat}} \cdot \int_{s < \Delta\sigma} D_{fat}(s) \cdot ds \tag{4}$$

As can be seen, only the upper 25 % of all stress ranges contribute significantly to the fatigue damage, while the upper 5 % account for 80 % of the fatigue damage. Hence, especially the stochastic description of the very high stress ranges is important for the probabilistic fatigue design.

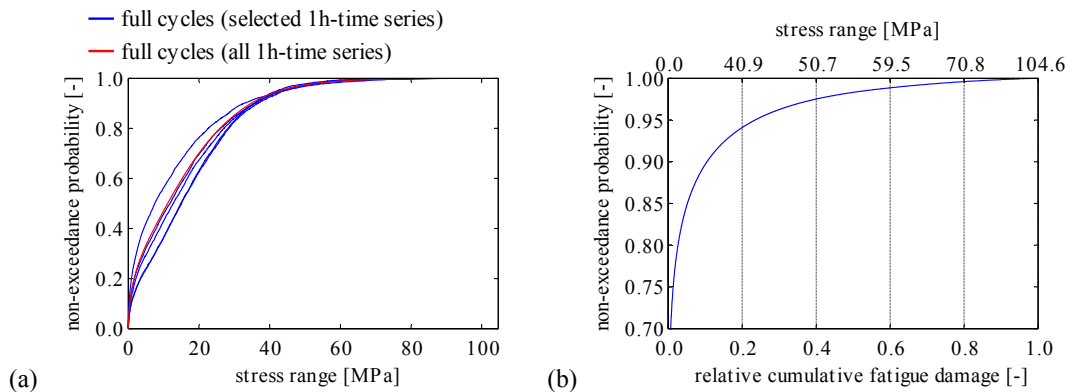


Fig. 3. (a) Empirical cumulative distribution function of full cycles; (b) cumulative fatigue damage of full cycles.

5. Probabilistic fatigue design

For probabilistic description on basis of data, these data must be independent and identically distributed. Evaluation of the autocorrelation function applied on the time series by means of the average lag of first zero-crossing indicate that uncorrelated data are available every 10 to 15 seconds, meaning that only 240 to 360 independent and identically distributed random data points exist within a time series of 3600 seconds. However, it is stated that less than 5 % of the upper, independent and identically distributed random variables can be used for the

description of the very high, rarely occurring values of a probability distribution [14]. For this purpose, only less than 12 to 15 values per 3600 seconds can be used, justifying the high number of time series simulated.

5.1. Statistical behavior of the very high stress ranges

For the tail estimation of a probability distribution, covering the very high, rarely occurring values, the peak-over-threshold method is used. The method is well established in other disciplines such as hydrology or finance mathematics. General and further information are given by e.g. Embrechts et al. [14].

By definition, the distribution above a certain threshold u is described by the generalized Pareto distribution (GPD). The respective probability density functions of the GPDs are

$$f_{\xi, \beta, u}^{GPD}(x) = \begin{cases} \frac{1}{\beta} \cdot \left(1 + \xi \cdot \frac{x-u}{\beta}\right)^{-\frac{\xi+1}{\xi}} & \text{if } \xi \neq 0, \\ \frac{1}{\beta} \cdot \exp\left(-\frac{x-u}{\beta}\right) & \text{if } \xi = 0, \end{cases} \quad x \in D(\xi, \beta, u) \tag{5}$$

with the domain of definition D depending on shape parameter ξ , scale parameter β , and threshold u .

The values of threshold u , shape parameter ξ and scale parameter β are determined by applying the maximum-likelihood-estimation method (MLE method), which is suitable for GPDs with shape parameter $\xi > -0.5$, cf. e.g. [14]. The log-likelihood function L is given by

$$L((\xi, \beta); \mathbf{X}) = \begin{cases} -n \cdot \ln \beta - \frac{\xi+1}{\xi} \cdot \sum_{i=1}^n \ln \left(1 + \frac{\xi}{\beta} \cdot (x_i - u)\right) & \text{if } \xi \neq 0 \\ -n \cdot \ln \beta - \frac{1}{\beta} \cdot \sum_{i=1}^n (x_i - u) & \text{if } \xi = 0 \end{cases} \tag{6}$$

Eq. (6) is evaluated for all data x in the vector \mathbf{X} greater than the threshold u . The best fit of the data \mathbf{X} to the underlying GPD with previously chosen threshold u is found by finding the maximum of log-likelihood function L with respect to shape parameter ξ and scale parameter β . The MLE is carried out numerically.

For the upper brace of K-joint III, crown-bottom, the curves of shape parameter ξ and scale parameter β are shown in Fig. 4, as well as their respective 95 %-confidence interval, evaluating all 53 time series.

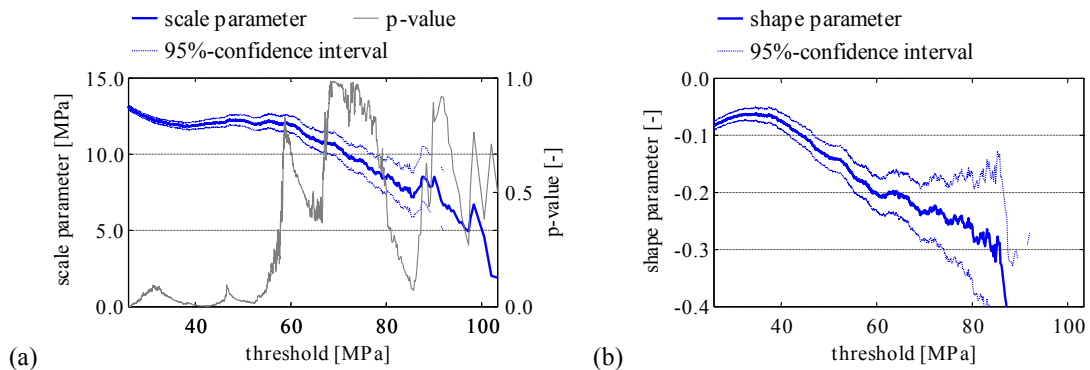


Fig. 4. Curves of (a) scale parameter and (b) shape parameter of GPD on basis of MLE for full cycles with respect to the threshold.

The Kolmogorov-Smirnow test is applied to determine the goodness-of-fit of the GPD with the parameters determined with the MLE method. In order to proof the null hypothesis that the data \mathbf{X} are described by the GPD with the parameters determined, the p-value is calculated. The p-value is the probability quantifying the strength of the evidence that the null hypothesis has to be rejected. The evidence not to reject the null hypothesis becomes stronger for greater p-values. The p-value with respect to the threshold u is plotted in Fig. 4 (a) (grey line).

Values for the thresholds $u = 60.0$ MPa and $u = 68.0$ MPa are chosen for p-values that are recognizably increased. In addition to the probability density function of the stress ranges obtained from the time series, the GPDs for both thresholds are shown in Fig. 5. Good agreement between the resulting GPDs and the distribution of the empirical stress ranges considered is given. The fatigue damage of the stress ranges greater than the respective threshold is nearly equal when evaluating either the empirical stress ranges or the GPDs by applying Eq. (3).

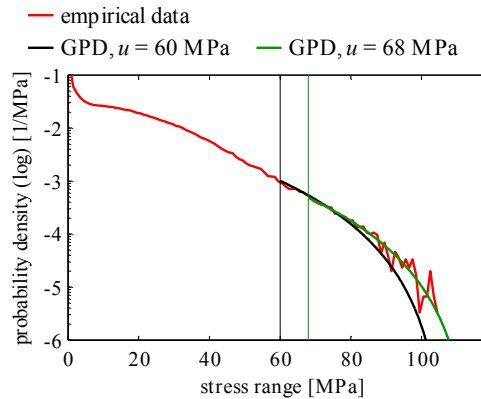


Fig. 5. Probability densities of full cycles, including the generalized Pareto distributions for the chosen thresholds

5.2. Remarks on the fatigue analysis of the very high stress ranges

The impact of the number of time series with a duration of 3600 seconds considered within the probabilistic fatigue analysis is shown in Table 1. All 53 numerically simulated time series as well as 60 random combinations of 6, 12, and 20 time series are evaluated concerning the probabilistic fatigue damage caused by the stress ranges greater than the chosen threshold u (here: $u = 60$ MPa) according to Eq. (3) as well as its statistical properties of mean value and (in italics) coefficient of variation. For reasons of comparison, the results are normalized for time series with a duration of 3600 seconds. For the very high stress ranges greater than the threshold u , the results are shown for the GPD of the stress ranges since no difference is noticed in the fatigue damage calculated by applying Eq. (3) on basis of either the stress ranges obtained from the time series or the GPD. Similar observations are found for a threshold of $u = 68$ MPa.

For the load case investigated, about 45-50 % of the fatigue damage is caused by the stress ranges greater than the threshold of $u = 60$ MPa which occur with a probability of about 1 %.

Table 1. Scattering of probabilistic fatigue damage, with a chosen threshold of $u = 60$ MPa.

no. of combined times series	no. of stress ranges $\Delta\sigma \geq u$	$D_{fat \Delta\sigma < u}$, Eq. (3)	$D_{fat \Delta\sigma \geq u}$, Eq. (3)	$D_{fat} / n_{ \Delta\sigma \geq u}$, Eq. (3)
1	0.370	4.673 $\cdot 10^{-6}$ 0.063	4.593 $\cdot 10^{-6}$ 0.438	0.166
6	0.130	4.692 $\cdot 10^{-6}$ 0.022	4.636 $\cdot 10^{-6}$ 0.146	0.034
12	0.095	4.664 $\cdot 10^{-6}$ 0.015	4.528 $\cdot 10^{-6}$ 0.105	0.023
20	0.062	4.686 $\cdot 10^{-6}$ 0.010	4.587 $\cdot 10^{-6}$ 0.071	0.017

mean value / coefficient of variation

Generally, accuracy of the fatigue damage increases with increased number of time series considered within the evaluation, as can be seen by the decreasing coefficient of variation. The mean value of the fatigue damage is almost constant. Further analysis shows that the fatigue damage of the very high stress ranges $D_{fat|\Delta\sigma>u}$ increases linear with the number of stress ranges considered while the fatigue damage caused by stress ranges less than the threshold u is constant independent of the number of stress ranges considered. The fatigue damage per each stress range greater than the threshold $D_{fat}/n|_{\Delta\sigma>u}$ is constant apart from scattering shown by the coefficient of variance. Hence, the number of the very high stress ranges has a significant impact on the respective fatigue damage.

6. Conclusions

Probabilistic fatigue analysis of offshore wind turbines is carried out for K-joints of a jacket substructure. Investigations have shown that especially the very high stress ranges are significant for the determination of the fatigue damage. The probability distribution of these stresses can be described by the generalized Pareto distribution. The peak-over-threshold method is applied. The method of maximum-likelihood estimation is used for determination of the respective probability function, leading to an accurate stochastic description of the very high stress ranges. Hence, significantly more values of the stress ranges are required for an accurate stochastic description of the very high, but rarely occurring stress ranges in comparison to the semi-probabilistic safety concept. This directly results in a significantly higher numerical effort. Also, the number of the very high stress ranges is to be estimated adequately and accurately.

Acknowledgements

This study has been carried out within the research project "Probabilistic Safety Assessment of Offshore Wind Turbines", financially supported by the Ministry for Science and Culture in Lower Saxony, Germany. The software used for fully-coupled simulations of OWTs consists of the software Flex5, provided by Servion SE, and the FE tool Poseidon. The Ministry for Science and Culture in Lower Saxony and Servion SE are kindly acknowledged.

References

- [1] DNV-OS-J101: Design of Offshore Wind Turbine Structures. Det Norske Veritas. Høvig, Norway; 2014.
- [2] Sørensen JD, Toft HS. Probabilistic Design of Wind Turbines. *Energies* 2010;3:241-17.
- [3] Hansen M (ed.). Probabilistic Safety Assessment of Offshore Wind Turbines - Annual Report 2013. Technical report, ForWind Hannover, Germany; 2014.
- [4] Thöns S. Monitoring Based Condition Assessment of Offshore Wind Turbine Support Structures. PhD thesis, ETH Zürich; 2011.
- [5] DNVGL-RP-0005: RP-C203: Fatigue design of offshore steel structures. DNV GL AS; 2014.
- [6] IEC 61400-3: Wind turbines - Part 3: Design requirements for offshore wind turbines. International Electrotechnical Commission. Geneva, Switzerland; 2009.
- [7] Vorpahl F, Popko W, Kaufer D. Description of a basic model of the "Upwind reference jacket" for code comparison in the OC4 project under IEA Wind Annex XXX. Technical Report, Fraunhofer Institute for Wind Energy and Wind System Technology. Bremerhaven, Germany; 2011.
- [8] Zwick D, Muskulus M. The simulation error caused by input loading variability in offshore wind turbine structural analysis. *Wind Energ.*; 2014. doi: 10.1002/we.1767
- [9] Joint Committee on Structural Safety. Probabilistic Model Code. Part III – Resistance Models. http://www.jcss.byg.dtu.dk/Publications/Probabilistic_Model_Code (accessed on Jan 9th, 2015); 2001.
- [10] Sonsino CM, Maddox SJ, Haagenen P. A Short Study on the Form of the SN-Curves for Weld Details in the High-Cycle-Fatigue Regime. IIW-Doc. no. XIII-2045-05; 2005.
- [11] Jonkman J, Butterfield S, Musial W, Scott G. Definition of a 5-MW Reference Wind Turbine for Offshore System Development. Technical Report NREL/TP-500-38060. NREL: Golden, CO, USA; 2009.
- [12] Efthymiou M. Development of SCF formulae and generalised influence functions for use in fatigue analysis. OTC'88: Proceedings of the Conference OTJ'88 on Recent Developments in Tubular Joints Technology. Surrey, UK; 1988.
- [13] Böker C. Load Simulation and Local Dynamics of Support Structures for Offshore Wind Turbines. PhD Thesis, Leibniz Universität Hannover. Aachen: Shaker Verlag; 2010.
- [14] Embrechts P, Klüppelberg C, Mikosch T. Modelling Extremal Events for Insurance and Finance. 4th ed. Berlin Heidelberg: Springer Verlag; 1997.